Journal of Hazardous Materials 423 (2022) 127161

Contents lists available at ScienceDirect

Journal of Hazardous Materials

journal homepage: www.elsevier.com/locate/jhazmat

Research Paper

Sea-level-rise-induced flooding drives arsenic release from coastal sediments

Fatemeh Izaditame [a,b,*], Matthew G. Siebecker [c], Donald L. Sparks [a]

[a] Department of Plant & Soil Sciences, University of Delaware, Newark, DE 19716, USA
[b] Department of Civil & Environmental Engineering, University of Delaware, Newark, DE 19716, USA
[c] Department of Plant and Soil Science, Texas Tech University, Lubbock, TX 79409, USA

ARTICLE INFO

Editor: Dr. C. LingXin

Keywords:
Climate change
Sea-level rise
Flooding
Arsenic release
Water pollution

ABSTRACT

Sea-level rise (SLR) has a vital influence on coastal hydrogeological systems, biogeochemical processes, and the fate of coastal contaminants. However, the effects of SLR-induced perturbations on the mobilization of coastal pollutants are not fully understood. In this study, the impact of SLR-induced flooding on the concentration and speciation of arsenic and selected hazardous chemicals is investigated using exceedingly contaminated sediments (5–6% As) collected from an urban coastal site in Wilmington, DE, USA. The release of contaminants from sediments was monitored before, during, and after flooding with different intensities (bottom shear stresses) through laboratory-based erosion chamber experiments. Significantly increased release of As (up to 150%) and NO_3 (up to 50%) from sediments at shear stress levels typically measured in estuaries were found. The release of toxic chemicals from contaminated coastal sediments is thus not restricted to extreme flooding events but can occur throughout the year. The results also suggest that the dissolved concentrations of pollutants continue to be considerably high even after the flooding. SLR-induced flooding can hence increase the release of contaminants not only during erosion events but over longer timescales. The release mechanism proposed here contributes to improving the risk assessment of coastal water pollution as climate change and SLR continue to occur.

1. Introduction

In many of the world's urban coastlines, sediments have turned into significant contaminant repositories and potential sources of pollution release to coastal water bodies (Ankley et al., 1996; Warnken et al., 2001). However, due to the multicomponent dynamic nature of coastal sediments, the fate of these coastal contaminants is unknown. Sea-level-rise(SLR)-induced flooding further complicates the prediction of coastal contaminant fate because it affects the biogeochemistry and physics of the sediments and overlying water (Borch et al., 2010). Given that nearly 40% of the global population inhabits within approximately 100 km of coastline (United Nations, 2007) and the fact that these populations are growing at twice the global average (Bijlsma et al., 1996), the impacts of SLR on the long-term fate of coastal pollutants are of environmental, economic, and ecological importance and expected to influence a large population. In recent years, climate change has increased the intensity and frequency of extreme weather events and raised the global mean sea level, resulting in increased flood risks (Hoozemans et al., 1993; Bijlsma et al., 1996). By 2100, this pattern is expected to continue, and extreme sea levels that were once historically rare will become common, leading to severe flooding in global coasts (IPCC, 2021). Such hydrologic changes will certainly influence existing contaminations along the coasts; yet, the mechanism and extent of the impact are not fully understood.

The physical disturbances caused by flooding can increase the diffusive flux of contaminants at the sediment-water interface (SWI) by more than an order of magnitude (Lorke et al., 2003; Wengrove et al., 2015), mobilize sediments into the water column (i.e., cause sediment resuspension), and facilitate the transport of resuspended contaminants away from their original site of deposition. Sediment resuspension further changes the chemical environment experienced by particles when they are eroded from anoxic bed sediments and enter the oxygenated overlying water (Saulnier and Mucci, 2000; Eggleton and Thomas, 2004). Such changes in the oxygen level threaten to release redox-sensitive toxic elements such as arsenic (As) into the water. The fate and bioavailability of metal(loid)s such as As are therefore regulated by the potential oxidation of anoxic sediments, metal sulfides, and reduced iron (Fe) and manganese (Mn) throughout flooding and

* Corresponding author at: Department of Plant & Soil Sciences, University of Delaware, Newark, DE 19716, USA.
E-mail addresses: fizadi@udel.edu (F. Izaditame), Matthew.Siebecker@ttu.edu (M.G. Siebecker), dlsparks@udel.edu (D.L. Sparks).

https://doi.org/10.1016/j.jhazmat.2021.127161
Received 14 April 2021; Received in revised form 31 August 2021; Accepted 4 September 2021
Available online 11 September 2021

resuspension (Klinkhammer et al., 1982; Shaw et al., 1990; Morse, 1994; Simpson et al., 1998, 2000; Chen, 2004; Bushey, 2008).

To predict the fate of sediment-bound contaminants during flooding and resuspension, it is crucial to consider and understand both the chemical (i.e., sediment and water (geo)chemistry) and physical (i.e., local hydrodynamics and sediment erodibility) processes impacting the sediments. On the physical side, although much research has been conducted on quantifying the release of contaminants under quiescent conditions, the release and speciation of pollutants during turbulent flooding conditions in historically contaminated coastal sediments, is not well understood. In addition, while prior studies have focused on the chemical processes affecting pollution mobilization during flooding (e.g., Cantwell et al., 2002, 2008; Kalnejais et al., 2007, 2010; Wengrove et al., 2015), the corresponding behavior of anionic and cationic pollutants has not been resolved. Overall, the current literature lacks an integrated investigation tailoring both chemical and physical aspects acting on pollution release under turbulent flooding conditions. To address this knowledge gap, the current study examines the chemical and physical impacts of flooding and sediment resuspension on the release of anionic (i.e., As and NO_3) and cationic (i.e., NH_4, Co, Ni, Mg, Mn, Pb, and Zn) pollutants from a contaminated site in coastal Wilmington, DE, which is a densely populated coastline expecting about 1 m of SLR by 2100 (Love et al., 2013). Particularly, in the current study, the behavior of As, as a highly concentrated and toxic element, is detailed during flooding.

Even though As is one of the most prevalent toxic elements in the environment, the concurrent variations in As release and speciation over the range of shear stresses that occurs in the natural environment have not yet been assessed. The labyrinthine world of As toxicity, mobility, and fate in the environment is defined by a complex series of controls dependent on the environmental conditions, chemical speciation, and biological processes. Here, to unravel the complex nature of As behavior during turbulent flooding conditions, we focused on the impacts of changes caused by flooding on the release and speciation of As. To that end, a laboratory-based sediment erosion chamber (EROMES) was employed to impose a series of various shear stresses ranging from quiescent to extreme storm conditions that are typically encountered in coastal environments. The concurrent physical and chemical impacts of moderate to extreme flooding on the release and speciation of As and selected elements are quantified in this novel combination of experimental conditions for the first time. Such information provides new insights into the processes controlling the long-term fate of pollutants in contaminated and tidally impacted coastal sediments affected by climate change and SLR. The data from this research plays a crucial role in developing accurate speciation and transport predictive models to understand how climate change affects the cycling of contaminants in polluted coastal sediments.

2. Experimental section

2.1. Sediment sampling and characterization

Sediment samples were collected from a highly contaminated coastal site in Wilmington, DE, projected to be inundated by 1 m of SLR by 2100 (see Fig. S1). The site is adjacent to the Christiana River, along the banks of a tidally-influenced ditch constructed as part of a remediation effort for a neighboring U.S. EPA superfund site, and it floods periodically from the Christina River and urban runoff. Three groups of surface sediments with different chemistries were collected from the lower (LDS) and upper (UDS) portions of the tidal ditch and the Christiana riverbank (RBS). Extremely high As levels (50,000–60,000 mg kg^{-1}) were located in the ditch sediments. Fig. S2 is an example of the collected ditch sediments. Table 1 and Table 2 summarize the chemical properties and elemental composition of the collected sediments, respectively. The sediments are characteristic of the area, with a history of tannery, chemical production, and ore processing contamination. We note here that extremely high As levels (30,000 mg kg^{-1}) were also previously reported in this location (e.g., LeMonte et al., 2017).

Table 1
Chemical properties of collected sediment samples.

Properties	Unit	RBS	UDS	LDS
pH	—	6.9	6.2	6.1
OM by LOI	%	2	8.5	8.2
Total N	%	0.10	0.30	0.32
Total C	%	4.30	4.40	4.80
CEC-pH 7.0	meq/100 g	7.6	52.0	50.5
Sand	%	51	34	36
Silt	%	35	47	49
Clay	%	14	19	15
Texture	—	Loam	Loam	Loam

Table 2
Elemental composition of collected sediment samples.

Element (mg kg^{-1})	RBS	UDS	LDS
Al	9370	10,200	12,400
As	800	60,000	51,000
B	5	8	9
Ca	5600	8500	7800
Cd	5	4	6
Co	430	185	260
Cr	50	30	40
Cu	4700	55	75
Fe	103,900	195,500	179,400
K	1500	1750	2000
Mg	2900	4300	5200
Mn	320	430	500
Na	490	770	680
Ni	100	90	120
P	390	1150	1400
Pb	13,900	1300	1900
S	6330	2390	2630
Zn	1700	4900	5700

Sediment samples were further sieved through a 4 mm sieve and stored at 4 °C with ca. 2 cm overlying water in the dark until experiments were conducted. Sediment pH_{water}, texture, cation exchange capacity (CEC), total C and N, and organic matter were measured using standard methods (Sparks et al., 2020) (see Table 1). Total arsenic and selected elemental content of the homogenized samples were determined by microwave-acid digestion (Agency, U. S. E. P., 1998), followed by analysis via inductively coupled plasma atomic emission spectrometry (ICP-AES, Thermo Elemental Intrepid II XSP Duo View) (see Table 2). X-ray diffraction (XRD) analysis of dried sediments was carried out using a Perkin Elmer XRD1621 flat panel with 200 μm pixels in 2048 × 2048 array at beamline 4-BM, National Synchrotron Light Source II (NSLS-II), Upton, NY with an incident wavelength of $\lambda = 0.8856$ Å (E = 14 keV). The patterns were collected in transmission geometry. Semi-quantitative XRD analysis using the reference intensity ratio (RIR) method was performed in the computer program Match! version 3.11.3.192.

Sediment samples were then centrifuged to extract pore waters. Extracted pore water samples were filtered through 0.45 μm Millipore nylon membrane filters (Whatman, Inc) and analyzed for selected elements (see Table S1). Three-gallon carboys were filled with the Christina River water to be used in the experiments. Water samples were filtered through 0.45 μm filters and stored at 4 °C in the dark until experiments were conducted. pH, electrical conductivity (EC), ammonium (NH_4), nitrate (NO_3), total inorganic carbon (TIC), total organic carbon (TOC), total carbon (TC), and selected elements and metals aqueous concentrations were measured in the quadruplicate water samples using mentioned standard methods (see Table S2).

2.2. Experimental set-up

A modified EROMES (see Fig. 1) erosion chamber (Tolhurst et al., 2000; Kalnejais et al., 2007, 2010; Wengrove et al., 2015; Percuoco et al., 2015) was employed for all experiments to quantify the release of As and selected elements (i.e., NO_3, NH_4, Co, Ni, Mg, Mn, Pb, and Zn) from sediments due to resuspension induced by shear stress (i.e., flooding). EROMES is among the most precise laboratory devices capable of simulating the flooding conditions typically encountered in coastal environments ranging from quiescent to extreme storm conditions (Gust and Müller, 1997). To impose shear stress at the SWI, EROMES uses an impeller and baffles within the core barrel. Turbulence is generated by a stainless-steel propeller coated with Teflon mounted 3 cm above the sediment while the baffles suppress the full body rotation of the water column. Sieved sand and Shield's erosion threshold curve were used to calibrate the chamber (Kalnejais et al., 2007). The detailed geometry and calibration of the chamber are represented in Kalnejais et al. (2010, 2007), respectively.

In this study, three sets of experimental systems were set up using different sediments (i.e., RBS, UDS, and LDS). Each experiment had three different phases (see Fig. 1): (1) pre-erosion phase (i.e., benthic flux measurements) to measure the release of elements in quiescent or no-flow/no-shear-force conditions; (2) erosion phase to simulate the release of elements in turbulent conditions with different agitation intensities; and (3) post-erosion phase to measure the elemental release over time after stopping the shear force (i.e., flooding). Each experiment is named after the sediment that is used in that specific experiment. In each phase, water and suspended sediment samples were collected from the erosion chamber at specific time points by sampling using a peristaltic pump from 2 cm above the SWI. Collected water samples were then filtered through 0.45 μm filters and divided into a 2 mL and a 48 mL portions for As speciation analysis using HPLC/ICP-MS, and elemental composition analysis via inductively coupled plasma atomic emission spectrometry (ICP-AES, Thermo Elemental Intrepid II XSP Duo View), respectively. The detection limit for the measured elements is 0.01 mg L^{-1}, with an average reproducibility better than 3%. The portions for solution speciation analysis were immediately frozen, and the 48 mL portions were refrigerated at 4 °C until analysis with ICP-AES. The schematic diagram of each of the experiments is demonstrated in Fig. 1. More details about each phase and sampling procedure can be found in Supplemental Text 1.

3. Results & discussion

3.1. Natural sediments & water characteristics

3.1.1. Natural sediment characteristics

Despite being collected from adjacent areas, ditch (UDS and LDS) and riverbank (RBS) samples had distinct geochemical compositions with different contamination levels. The chemical properties and elemental composition of sediments are summarized in Table 1 and Table 2, respectively. Strikingly, more than 5% As was found in the UDS and LDS (see Table 2). Arsenic, Fe, Mg, and P were enriched in the UDS and LDS compared to RBS, while RBS was more enriched in Co, Cu, S, and Pb, where Pb > S > Cu > Co. Sediment samples had relatively neutral pH, with UDS and LDS having, on average, slightly lower pH (6.2 and 6.1, respectively) than that of RBS (6.9). The organic matter contents of UDS and LDS were almost four times higher than RBS. The average TOC concentrations and the cation exchange capacities (CEC) of UDS and LDS were also higher than RBS, while the C:N ratios of RBS were almost three times larger than UDS and LDS.

The textural class of the sediments was loam with a mud fraction greater than 50%. These sediments are cohesive with the high mud fraction, and diffusion dominates the transport rather than advection (Boudreau, 1997). The semi-quantitative results of XRD (see Fig. S3) demonstrated the existence of quartz (SiO_4 = 36.7%), hematite (Fe_2O_3 = 58.8%), and jarosite ($Fe_3H_{12}KO_{14}S_2^{-3}$ = 4.5%) in RBS. Additionally, UDS and LDS consisted of quartz (SiO_4 = 90.5%), goethite (FeOOH = 4.1%), scorodite ($FeAsO_4.2H_2O$ = 5.1%), and tooeleite ($Fe^{3+}{}_6(As^{3+}O_3)_4(SO_4)(OH)_4\ 4H_2O$ = 0.4%).

3.1.2. Collected water and porewater properties

For all three sediments, interstitial water concentrations were below detection limits for Al (< 0.05 mg L^{-1}), Cr (< 0.003 mg L^{-1}), and (P < 0.025 mg L^{-1}) and measurable for As, Fe, Co, K, Mg, Mn, and Zn (see Table S1). Arsenic, Co, Fe, Ni, and Zn in the porewaters of the UDS and LDS were higher than RBS, while Cd, Cu, Mg, Mn, Pb, and S concentrations were higher in the RBS. Duplicate river water samples were analyzed two times (reported as a and b) for the chemical properties (see Table S2). Aluminum (< 0.03 mg L^{-1}), As (< 0.01 mg L^{-1}), Cd (< 0.002 mg L^{-1}), Cr (< 0.002 mg L^{-1}), Cu (< 0.005 mg L^{-1}), P (< 0.025 mg L^{-1}), and Pb (< 0.015 mg L^{-1}) were below the detection limit of the ICP instrument in the river water.

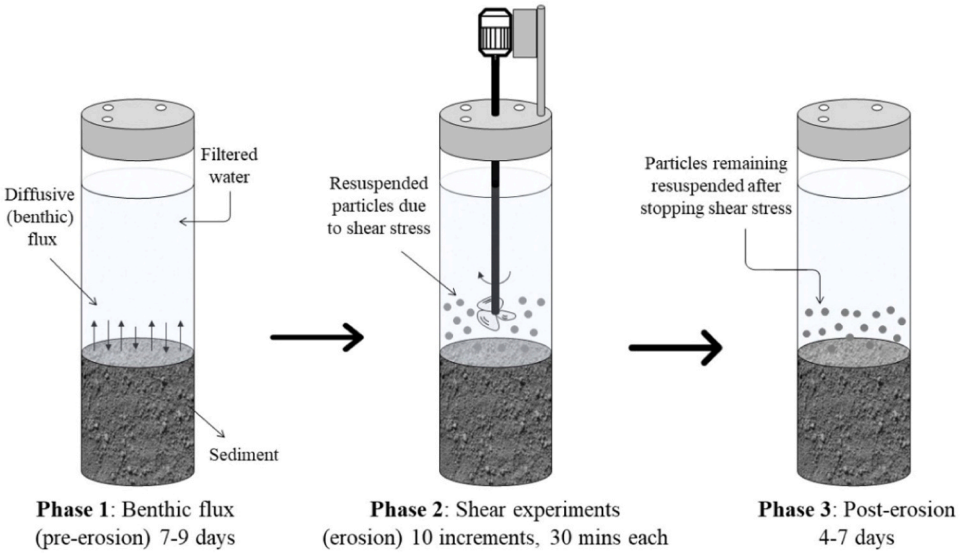

Fig. 1. Schematic diagram of pre-erosion, erosion, and post-erosion phases. These three phases were present in all three experiments in which Riverbank Sediment (RBS), Upper Ditch Sediment (UDS), and Lower Ditch Sediment (LDS) were used. The schematic shows only one experiment as a model for the other two.

3.2. Phase 1: pre-erosion (benthic flux) results

Fig. S4 illustrates the alterations in chemical composition (i.e., pH, EC, Eh, and the concentrations of As, NO_3, and NH_4) of the overlying water during the pre-erosion phase (i.e., phase 1) of the RBS, UDS, and LDS experiments. In the overlying solution, the pH and Eh remained almost constant during phase 1 in all experiments, while EC slightly declined. During this phase, the concentrations of As and NO_3 generally increased, as opposed to NH_4, which declined. Also, As aqueous concentrations ranged from 10 to 15 μg L^{-1} in the RBS experiment during phase 1, but drastically different results were observed for the experiments on LDS and UDS. For these experiments (i.e., LDS and UDS), the initial dissolved As concentrations were between 5 and 20 μg L^{-1}, and increased to 45 and 65 μg L^{-1} over four and six days, respectively. Arsenic concentration in the original RBS (800 mg kg^{-1}) is much lower than in the UDS (60,000 mg kg^{-1}) and LDS (51,000 mg kg^{-1}) (see Table 2), which explains why aqueous As concentration increased in the experiments involving UDS and LDS. In addition to monitoring the changes in As aqueous concentration, As speciation analysis was also carried out on the collected water samples in this phase (see Fig. S5). Speciation in solution showed that As was mostly in As(V) oxidation state during phase 1 in all experiments. As plotted in Fig. S6, the

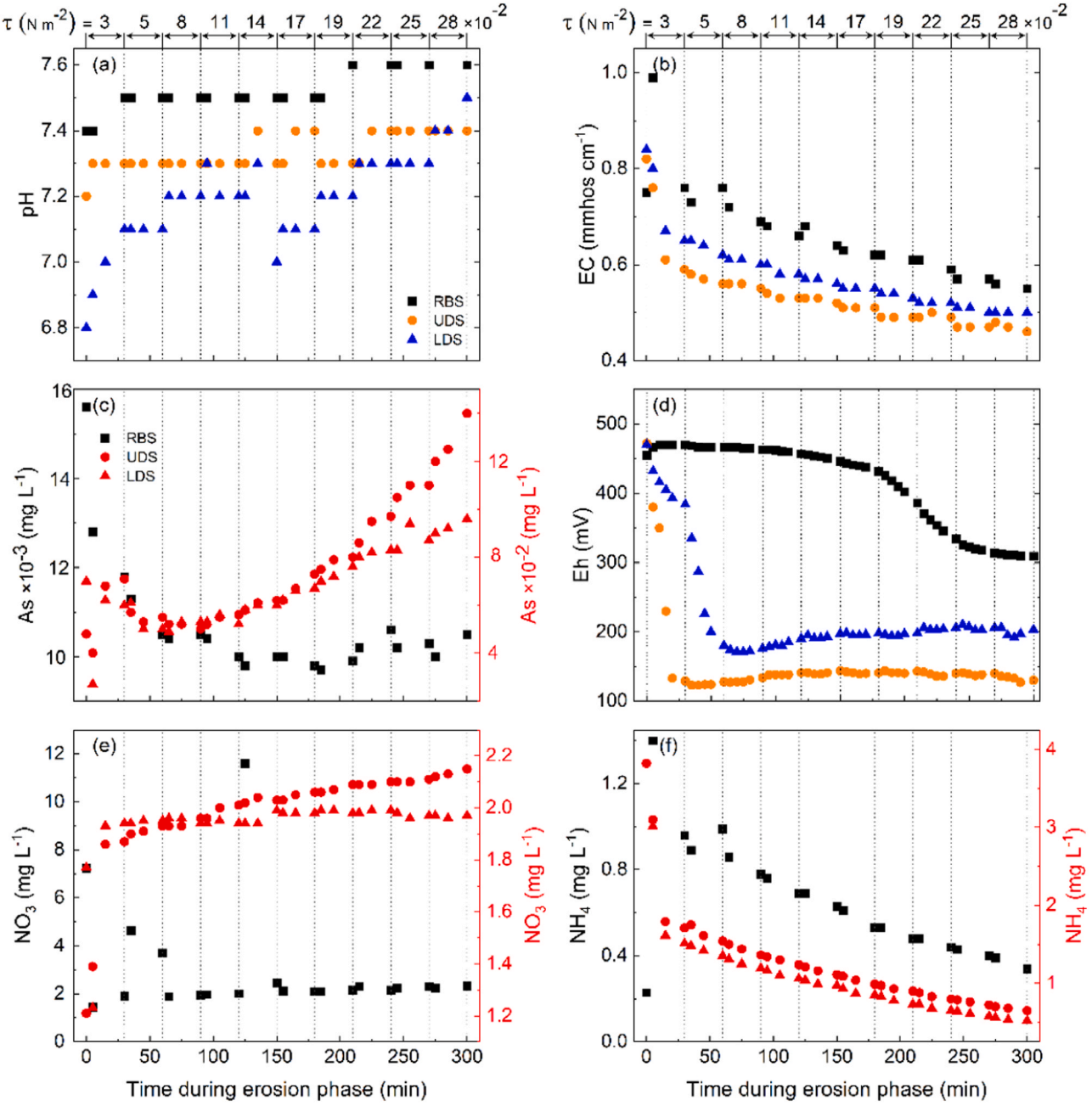

Fig. 2. Changes in the pH (a), EC (b), As concentration (c), Eh (d), and the concentrations of NO_3 (e) and NH_4 (f) during the erosion phase of RBS (square), UDS (circles), and LDS (triangles) experiments over time (bottom x-axis) and different shear stress levels (top x-axis). The average reproducibility of the measured parameters is better than 3%. $\tau = 11 \times 10^{-2} Nm^{-2}$ is the critical shear stress value. Black, orange, and blue colors represent data for RBS, UDS, and LDS in single-Y axis graphs. Black and red colors represent the data in double-Y axis graphs. For the sake of comparison, the double-Y axis is used when the concentration of a species was significantly different in one of the experiments. (For interpretation of the references to colour in this figure legend, the reader is referred to the web version of this article.)

concentration of cationic elements (i.e., Co, Ni, Mg, Mn, Pb, and Zn) generally decreased during the pre-erosion phase of all experiments. The changes in concentrations during phase 1 can be partially attributed to in/out fluxes of porewater chemicals due to diffusion and/or adsorption/desorption processes.

3.3. Phase 2: erosion (shear stress) results

3.3.1. Solute release

For the first shear stress increments ($\tau < 0.1 \mathrm{Nm}^{-2}$), no resuspension of particles into the overlying water was observed. Starting from the shear stress of 0.11 N m^{-2}, however, a significant release of particles in all experiments caused the water column to become turbid and cloudy. This point is the critical shear stress (τ_c) for which the imposed stress exceeds the cohesive forces within the sediment. Beyond τ_c the eroded mass increases steadily with shear stress. Specifically, our analysis indicated that the release of solutes is a function of the magnitude of imposed shear stress at the SWI. However, at each shear stress, the behavior of different species is less sensitive to the duration of shear stress. For example, in the UDS experiment, the aqueous As concentration increased slightly by 12% after applying constant shear stress of $\tau = 0.28$ Nm^{-2} for 30 min compared to a 5-minute application of the same stress. Also, only a 1.5% increase was observed over the same period for NO_3 aqueous concentration (see Fig. 2). The low sensitivity of different species to the duration of stress application suggests that the majority of the release/scavenging processes occur rapidly, and thus, 30-min shear stress time intervals are adequate to determine the total release at particular shear stress.

The temporal changes in pH, EC, Eh, and the concentrations of As, NO_3, and NH_4 with shear stress are presented in Fig. 2. In all experiments, increasing bottom shear stress increased the pH of the overlying water. Moreover, a sharp removal of Fe from solution (to below detection limit) was observed right after applying the first shear stress. Even though Fe concentration decreased in solution, a combination of reductive dissolution of Fe oxides in the bed sediment and microbially mediated Fe(III) reduction in solution potentially govern the observed increase in pH. The EC, on the other hand, decreased with increasing bottom stress (see Fig. 2). We attribute the decrease in EC to the scavenging of cationic species from the solution. For redox potential, all experiments behaved similarly with an overall drop in Eh with shear stress, where the observed drops were more pronounced for the UDS and LDS experiments than the RBS (see Fig. 2). The UDS and LDS (original sediments) have more OM than the RBS (see Table 1), which provides an abundant carbon source for microbial respiration. This likely contributed to the large difference in the rate of Eh drop between the RBS and UDS/LDS experiments.

We found that the concentration of anionic species (i.e., As and NO_3) generally increases with increasing bottom stress (see Fig. 2-c and -e). During the erosion phase, in general, aqueous As concentrations showed a consistent trend for all experiments with an initial drop for $\tau < \tau_c$ followed by a slow (for RBS) or an acute (for UDS and LDS) increase for $\tau > \tau_c$. The release pattern likely depends not only on the applied bottom stress but on the amount of As in the original sediment. Specifically, for the RBS experiment, where As concentration is only about 1.5% of the UDS and LDS (see Table 2), As concentration had a ca. 40% decrease in the solution when shear stress gradually increased from 0 to 0.28 Nm^{-2}. After reaching τ_c, however, the alterations in aqueous As concentration became stable and slightly rising (see Fig. 2-c). In the UDS and LDS experiments, even though a slight initial decrease in dissolved As concentration was noticed before τ_c, the overall As concentration in solution increased 250% (UDS) and 92% (LDS) with incrementally increasing bottom stress from 0 to 0.28 Nm^{-2}. When $\tau < \tau_c$, smaller particles dominate the size distribution; therefore, scavenging may be enhanced due to higher particle surface areas, yielding a smaller release in lower τ values. This explains the slight decrease in As concentration up to $\tau_c =$ 0.1 N m^{-2}. At higher shear stress levels, however, deeper sediments are eroded, thus more As and reduced phases become liberated. More metals are hence released at higher shear stresses due to the potential for the release of minerals that have been impacted by reductive dissolution.

Arsenic speciation in solution at the end of each shear stress increment is shown in Fig. 3. Arsenate (As(V)) was the dominant aqueous As species in all experiments. In sediments, groundwater, and soils, the As (V) species predominates under oxidizing and aerobic conditions, while the As(III) species predominates under reducing conditions (Sadiq et al., 1983; Korte and Fernando 1991; Cherry et al., 1979). Therefore, it is predictable to have more As(V) species in the solution when anoxic sediments get oxidized after being resuspended. On the other hand, the As(III) species tends to be more weakly bound to soils and sediments and, therefore, would be more mobile than As(V). For that reason, having more As(V) in the solution rather than As(III) can be due to the presence of As(V) in colloidal (instead of soluble) form. The reader is referred to Section 3.3.3 for further details.

In all experimental conditions, the concentration of NO_3 increased with increasing shear stress while NH_4 concentration declined. The observed increasing pattern for NO_3 concentration was more significant in the UDS and LDS than the RBS experiment (see Fig. 2-e, f). Inorganic nutrients release in quantities greater than the sole entrainment of porewater were also reported by, for example, Kalnejais et al. (2010), Couceiro et al. (2013), and Percuoco et al. (2015). The enhanced NO_3 release can be because of the stimulation of nitrification or desorption from resuspended sediments that were at equilibrium with porewater concentrations (Couceiro et al., 2013; Kalnejais et al., 2010). To elaborate more on this, the correlation between As and TIC/TOC (Figs. S7-a,b, c) and As and NO_3/NH_4 (Figs. S7-d,e,f) aqueous concentrations in the UDS and LDS experiments were further investigated. As it is shown in Fig. S7, the concentration of TOC and NH_4 dropped when As concentration increased in the solution by increasing shear stress. The concentration of TIC and NO_3, on the contrary, both increased when As concentration in the solution increased with enhancement of the shear stress at the SWI. The correlations among NO_3, NH_4, TOC, and TIC concentrations shed light on the potential role of microbial activities in the observed variations in NO_3 concentration when sediment is imposed to shear stress. Moreover, the observed correlations between As, NO_3, and NH_4 concentrations further emphasize that nitrogen cycling can conceivably be correlated to As release and speciation during flooding. Therefore, As release and nitrogen cycling can be likely affected by

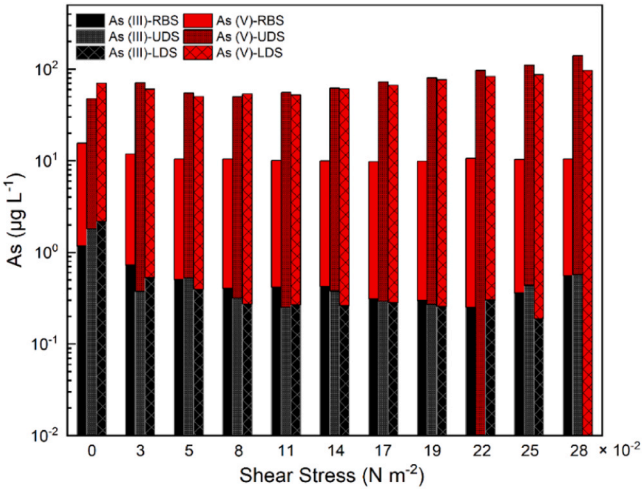

Fig. 3. The speciation of As in solution during the erosion phase of the RBS (black/red), UDS (dotted black/red), and LDS (hashed black/red) experiments at different shear stress increments. The average reproducibility of the measured As concentrations is better than 3%. Y-axis is reported in log scale to compare As(III) and As(V) concentrations with ca. an order of magnitude difference. (For interpretation of the references to colour in this figure legend, the reader is referred to the web version of this article.)

climate change as a major factor contributing to SLR-induced flooding.

The variations in the concentrations of cationic species (i.e., Co, Ni, Mg, Mn, Pb, and Zn) with shear stress are plotted in Fig. S8. Overall, the concentrations of cationic species slightly increase at lower shear stresses (i.e., $\tau < \tau_c$) and then decline with increasing the stress (see Fig. S8). Specifically, the concentrations of Co, Mg, Mn, Ni, Pb, and Zn initially increased in the solution in the RBS experiment (at $\tau = 0.03$ N m^{-2}) before declining with further increasing the bottom stress. Lead remained below the detection limit in the UDS and LDS experiments, but in the RBS experiment, it displayed an initial increase (up to $\tau = 0.05$ N m^{-2}, i.e., prior to the erosion threshold) followed by a decline that is potentially due to an affinity for the solid phase. The concentration of Fe in the solution was also measured for all experiments, and a sharp drop in soluble Fe concentration to below the detection limit was observed at the onset of applying the lowest shear stress. The oxidation of Fe(II) is rapid (Roekens and Grieken, 1983) compared to the timescale of our experiments. The fast decline in aqueous Fe concentration in these experiments can, therefore, indicate the formation of Fe precipitates or sorption of Fe to solids.

Interestingly, our results showed that significant variations in the concentrations of anionic and cationic species occur at low shear stresses below τ_c, after which the changes in the concentration of different species are less sensitive to increasing shear stress (see Fig. 2, and Fig. S8). This significant result underscores the importance of more frequent, low-intensity flooding events on the release of pollutants in contaminated areas. Regardless of the release mechanism, the steep concentration changes at low shear stresses emphasize the impact of flooding and sediment resuspension on remobilizing contaminants (particularly As and NO_3) from coastal sediments. Substantial release due to sediment resuspension does not hence require large storm events but happens at shear stresses with magnitudes that occur regularly, such as spring tides. Low shear stress events are disproportionately important due to their frequent occurrence, and so the release of anionic elements such as As and NO_3 can be a vital part of remobilization in contaminated coastal environments.

3.3.2. *The mechanisms of solute release/scavenging during erosion experiments*

The observed changes in the concentrations of dissolved species during the erosion phase can be originated from (1) advective/diffusive flux of pre-existing dissolved species from the sediments, (2) reactions of particles within the bed sediments, and/or (3) reactions of particles suspended in the water column (i.e., desorption from resuspended particles). In our experiments, advection does not govern the release of As and NO_3 from these cohesive sediments with a high mud fraction where diffusion dominates transport rather than advection. Diffusion also cannot be the primary mechanism contributing to the released species because the concentration of released species in the water column is greater than the low equilibrium porewater values (see Fig. 2, Fig. S8, and Table S1). The porewater contribution was calculated following Kalnejais et al. (2007) from the porewater concentrations in Table S1, the measured sediment porosity (i.e., 0.44, 0.43, and 0.52 in RBS, UDS, and LDS experiments, respectively), and the calculated erosion depth (~2 cm) for each shear stress level. Release in excess of porewater contributions was also reported by, for example, Cantwell et al. (2002), Kalnejais et al. (2010), Percuoco et al. (2015), and Wengrove et al. (2015). The reaction of particles within the bed sediment is also unlikely to be the source of As release. In the RBS experiment, for instance, the soluble As concentration declined with increasing shear stress. Moreover, the depth profile of the digested RBS after erosion shows a decrease in the concentration of As at the surface of RBS compared to the original sediment (see Fig. S9). If the surface of the bed sediment were governing As behavior, an increase in the surface As concentration would be expected after the RBS erosion experiment, according to the conservation of mass. We conclude, therefore, that the solute release should be due to the reactions of the particles suspended in the solution during active erosion.

3.3.3. *Contributions from suspended particles*

In the previous section, the variations in the concentration of different species in the solution were mainly caused by the reaction of suspended particles. Here, further elaboration on the contribution of suspended particles to the observed fluctuations in the aqueous concentrations of cationic and anionic species is given. Throughout the erosion phase, the behavior of cationic species is in contrast with that of the anionic species because the release of cationic (anionic) species happens at lower (higher) shear stresses. The fact that the cationic species exhibited an exact opposite trend with shear stress indicates that a surface chemical reaction is likely governing the affinity of anions and cations for sorption sites on resuspended particles at different shear stress levels. The sorption/desorption of different species depends on the amount of the imposed shear stress and the nature and saturation of resuspended particles, which are in turn affected by the bottom shear stress. The saturation of resuspended particles is a potentially significant contributor to the observed release of anionic species at higher shear stresses, where the resuspended particles become incapable of further accommodating these released species over time.

At higher shear stress levels, increasing pH is another important factor affecting the sorption and removal patterns of different species. The high point of zero charge (PZC) of Fe oxides and the increase in pH over time potentially inhibits (oxy)anions sorption as the surface of resuspended particles becomes more negative. These negatively charged resuspended particles further become more favorable for cations to bind to as pH increases (see Fig. 2). That is when the release (removal) of anions (cations) in the solution initiates. An increase in pH and soluble As concentration was also reported by, for example, Yamaguchi et al. (2011). For oxyanions such as arsenate and arsenite with a tetrahedral structure, steric effects can also be responsible for the release at higher shear stress levels. It is perhaps easier for cations to approach the surface of an aggregate because they are smaller compared to tetrahedral structured oxyanions (Mobasherpour et al., 2012; Neil et al., 2014).

The enhanced release of dissolved As is also attributable to ion-exchange reactions. However, it is difficult to separate release due to ion-exchange processes from the release due to the reductive dissolution of Fe and Mn oxides in the sediments. The As associated with Fe and Mn oxides in the sediments is the most chemically reactive phase because the host phase can undergo redox shifts during flooding and resuspension. Reductive dissolution of Fe/Mn oxides is probable when sediments become saturated during flooding. On the contrary, oxidation is possible during the resuspension of anoxic sediments to the oxic overlying water (Morse, 1994; Simpson et al., 1998). In such a case, the reaction between ferrous iron in sediments and dissolved oxygen in the water column could oxidize the reduced Fe to form new solid-phase Fe oxides. The specifications of these high surface area metal oxides and their active binding sites make them capable of scavenging metals and removing them from the dissolved phase, hence reducing availability (Klinkhammer et al., 1982; Shaw et al., 1990). The balance between metal oxide dissolution and formation, both of which may occur during sediment resuspension, controls the fate and bioavailability of metals facing these types of environmental disturbances.

Given the elevated suspended particulate matter (SPM) levels and the physical alteration of particles by collision during resuspension, it is also expected that colloids were abundant and played a role in maintaining the concentration of As. This study measured colloidally-bound metals as part of the dissolved phase (< 0.45 μm). As we previously showed, As(V) is the dominant As species in the solution during the erosion phase of the current study (see Fig. 3); however, As(III) is generally dominant in the solution. Therefore, the observed increase in As(V) concentration in the solution may be in the colloidal form. This was also observed by Cantwell et al. (2002) and Kalnejais et al. (2010), in which they attributed high dissolved trace metal concentrations to the trace metal colloid complexes.

In addition to processes that lead to the release of solutes to the water column, removal processes such as scavenging were also active, especially for the cationic species. Processes such as adsorption and precipitation can effectively limit the amount of metal(loid)s and transition metals present in the water column over time. The exposure of new surface areas of suspended colloids, formed via collisions in suspension, with cationic species is the potential mechanism for removing cationic species during the erosion phase of the present study. These newly produced and negatively charged surface sites have a high potential to act as scavengers for cationic species in the solution.

3.4. Phase 3: post-erosion results

The changes in pH, EC, Eh, and the concentrations of As, NO_3, and NH_4 with time are illustrated in Fig. 4 for the post-erosion phase. The general trend of pH was different for each experiment (see Fig. 4-a); it showed an increasing (decreasing) trend for the RBS (LDS) experiment, while it was almost constant in the UDS experiment. However, the EC increased in all experiments indicating that the sorbed species during the erosion phase are likely releasing to the solution in the post-erosion phase (see Fig. 4-b).

Fig. 4-c shows that the As concentration considerably increases during the post-erosion phase for all experimental cases. For example, in the UDS experiment, As concentration almost doubled over 168 h. Early on, As concentration showed a sharp increase and reached its peak after about 48 h in all experiments. Arsenic concentration then decreased and reached a constant value at the end of the post erosion phase. Although As concentration decreased later on during the post-erosion phase, it remained considerably higher than the concentrations measured for phases 1 and 2. During the post-erosion phase, As concentration was, on

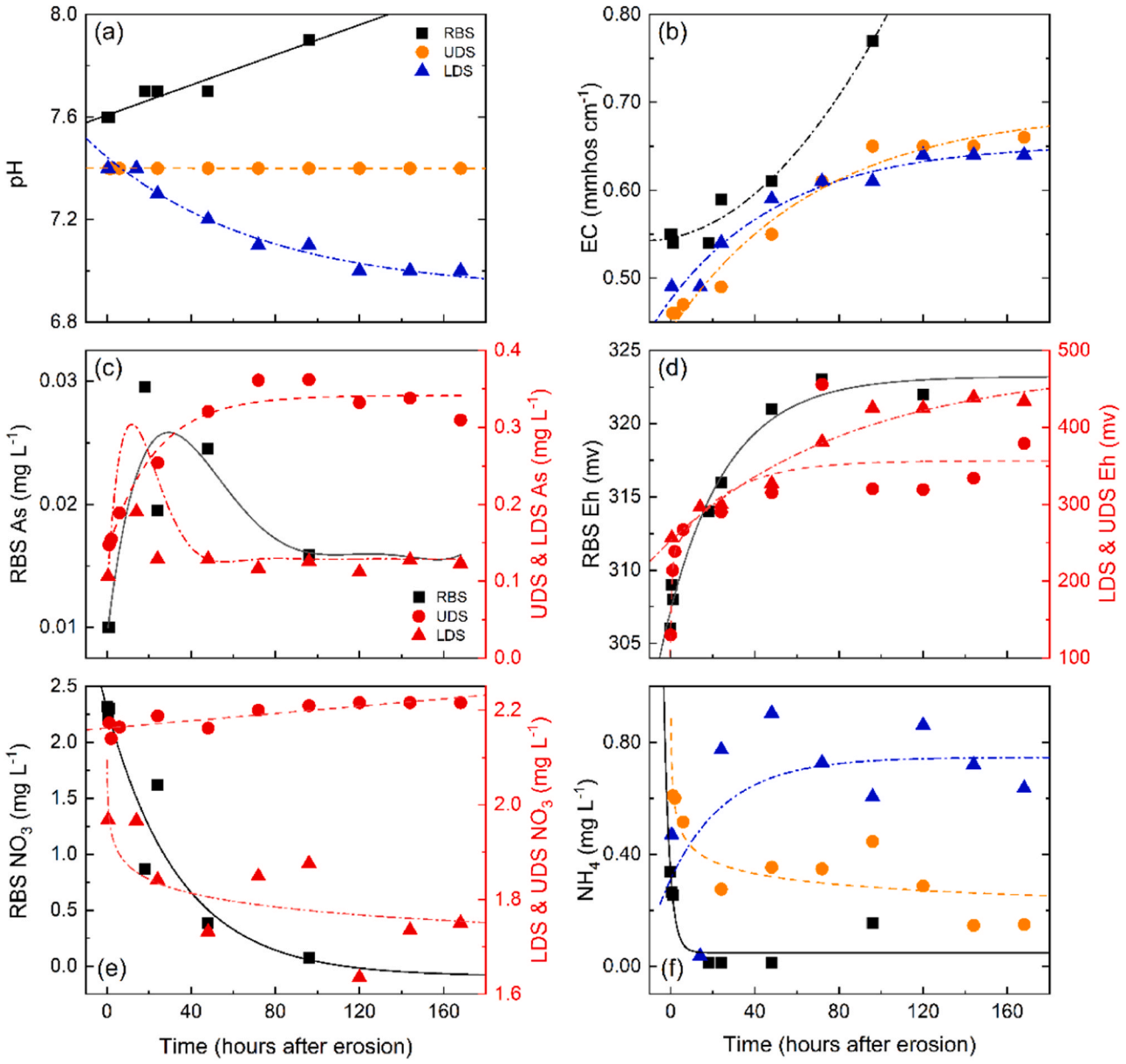

Fig. 4. Changes in the pH (a), EC (b), As concentration (c), Eh (d), and the concentrations of NO_3 (e) and NH_4 (f) during the post-erosion phase of RBS (square), UDS (circles), and LDS (triangles) experiments over time. The average reproducibility of the measured parameters is better than 3%. Black, orange, and blue colors represent data for RBS, UDS, and LDS in single-Y axis graphs. Black and red colors represent the data in double-Y axis graphs. For the sake of comparison, the double-Y axis is used when the concentration of a species was significantly different in one of the experiments. Lines show linear, polynomial, or exponential trendlines. The trend lines are used as a general aid to more clearly identifying changes in the data. (For interpretation of the references to colour in this figure legend, the reader is referred to the web version of this article.)

average, 1.5 (2), 12 (4), and 2 (1.5) times higher than that of post-erosion (erosion) phases for the RBS, UDS, and LDS, respectively. This is in part due to the release of the As species sorbed to the resuspended particles during the erosion phase. In addition, the concentration of Fe remained below the detection limit in the solution (i.e., < 0.05 mg L^{-1}) in all experiments during this phase. This indicates that desorption (rather than dissolution) is the predominant mechanism for increasing aqueous As concentration.

Even though the pre-erosion and the post-erosion phases were both stationary (i.e., without any exposure to shear stress), significantly different behavior concerning the release of As was observed in these phases. The significant increase in As concentration during the post-erosion phase was not observed during the pre-erosion phase, where the concentration remained primarily stable in the solution. This reveals the significance of the long-term impacts of erosion and flooding on the release of As from sediments to the overlying water. It is crucial to note that the speciation analysis for As in solution exhibited an increasing trend for As(III) formation in the post-erosion phase of the RBS and UDS experiments (see Fig. S10). The higher mobility of the As(III) compared to the As(V) explains the increase in As(III) concentration during active desorption of the post-erosion phase. Interestingly, As(III) formation was more significant in the RBS experiment with lower initial As concentration in the sediment (i.e., more representative of the common contaminated sites). The formation and increase in the aqueous As(III) concentration at the post-erosion phase of the LDS experiment was not observed. This indicates considerable heterogeneity in the collected sediments and probable slower chemical kinetics for the conversion of arsenate to arsenite in the LDS.

The Eh increased in the post-erosion phase and reached a plateau at the end of the post-erosion phase with values lower than that of the pre-erosion phase (see Fig. 4-d). It should be noted here that the system was not fully closed and was in contact with the air at its headspace in this phase. Fig. 4-e,f show the concentrations of NH_4 and NO_3 during the post-erosion phase. While both NO_3 and NH_4 decreased in the RBS experiment, NO_3 (NH_4) concentration decreased in LDS (UDS) and slightly increased in UDS (LDS). Contrary to the erosion phase in which the dissolved concentration of cations (i.e., Co, Mg, Mn, Na, Ni, Pb, and Zn) decreased, the aqueous concentrations of cationic elements increased in the post-erosion phase and, in most cases, exceeded the pre-erosion and erosion concentrations (see Fig. S11). Importantly, the water column stayed turbid in the post-erosion phase, showing the particles remained suspended over time scales of hours. According to Stokes' law for sedimentation of clays and nanoparticles, fine particles have a long residence time in the water column due to their size; sediment resuspension events can, therefore, result in the dispersal of pollution-enriched fine particles in natural waters. Part of this mobilized load will ultimately settle back to the estuaries and seafloors; however, the considerable fraction of particles that remain in suspension is highly enriched in pollutants and can be transported away from the source to water resources, finding their ways to the food web and human body.

3.5. Summary of pre-erosion, erosion, and post-erosion processes

Our results demonstrate that even though the sediment's chemical/physical composition is in concert with the level of applied shear stress at the SWI to affect the pollution release during flooding, the release/scavenging trends are quite similar for distinctly different sediments used in this study. Additionally, the cationic (anionic) contaminants release is more significant before (after) the critical shear stress. The evidence from this study further suggests that the concentrations of cationic and anionic pollutants can remain considerably high in solution even after the flooding events. Overall, we propose the following mechanisms for the behavior of As (vs. cationic pollutants) during SLR-induced flooding and resuspension: (1) short-term removal (vs. release) from (to) the solution at low flooding intensities due to scavenging (vs. desorption) by (from) eroded sediments, (2) sorption of cationic pollutants and saturation of resuspended particles at higher flooding intensities, (3) subsequent release of As to overlying water, (4) colloid formation and mobilization, and (5) release of As and cationic pollutants to water after flooding. The schematic of the proposed mechanism for As and cationic species behavior at different phases of the experiments are presented in Fig. 5.

4. Conclusions and environmental implications

The next several decades are likely to witness a considerable rise in sea levels accompanied by frequent and severe flooding events. An understanding of the fate and behavior of legacy coastal pollutants is, therefore, crucial in flood-prone contaminated coasts where geochemical conditions can alter due to climate change and SLR. In the current paper we outlined a new approach to quantify pollution release to coastal waters during SLR-induced flooding events. Monitoring three sets of experimental systems before (pre-erosion phase), during (erosion phase), and after (post-erosion phase) flooding events with different intensities (i.e., shear stress levels) allowed for a better understanding of the impacts of SLR-induced flooding on low-lying contaminated coastal sites and the fate of coastal contaminants.

We found a potential for a significant release of As and NO_3 from sediments at shear stress levels typically measured in estuaries. Substantial release of these contaminants due to sediment resuspension does not hence require large storm events but occurs at shear stresses with magnitudes that occur regularly. Therefore, sites with readily erodible particles and/or geochemical processes that trap trace metals in the surface layer can expect significant metal release even from the low-energy resuspension events. Notably, the released As during the erosion phase was approximately three orders of magnitude higher than the WHO and EPA limit for total As in drinking water (i.e., 10 μg L^{-1}). Here it is worth noting that such release was considerably greater than what porewater diffusion would solely contribute. Another important finding emerged from this study is that a considerable release of As (more than 80%) occurs during the post-erosion phase from the reactions of sediment particles that remain suspended. This suggests that pollution release due to resuspension should be considered in the long-term management of contaminated sediments. Even though As was mainly in As(V) oxidation state before, during, and after the flooding events, a significant increase in As(III) concentration was observed during the post-erosion phase. The importance of As(III) formation as the more mobile and toxic As species cannot be stressed enough; this is a vital issue for future research as it shows potential for an increase in As mobility, toxicity, and transport.

Overall, we conclude that the threat of SLR-induced flooding stands to adversely impact pollution release from contaminated coastal sediments. The results from this research constitute an important initial step toward understanding the impacts of SLR-induced flooding on the cycling of contaminants in coastal sediments and offer compelling evidence for the long-term release of As to overlying water due to SLR and flooding. These results are crucial for developing accurate speciation and transport predictive models to assess SLR-associated risks to water quality, design long-term monitoring approaches and pollution control guidelines, and prepare contingency plans for the climate-change-affected contaminated coasts. Additional laboratory and field-based investigations during turbulent flooding events are required to further understand the role of microbial communities and the kinetics and mechanisms of pollution release and removal during resuspension.

CRediT authorship contribution statement

Izaditame, Siebecker, Sparks: substantial contribution to conception and design. **Izaditame, Siebecker:** substantial contribution to acquisition of data. **Izaditame, Siebecker:** substantial contribution to analysis and interpretation of data. **Izaditame:** drafting the article. **Izaditame, Siebecker, Sparks:** critically revising the article for

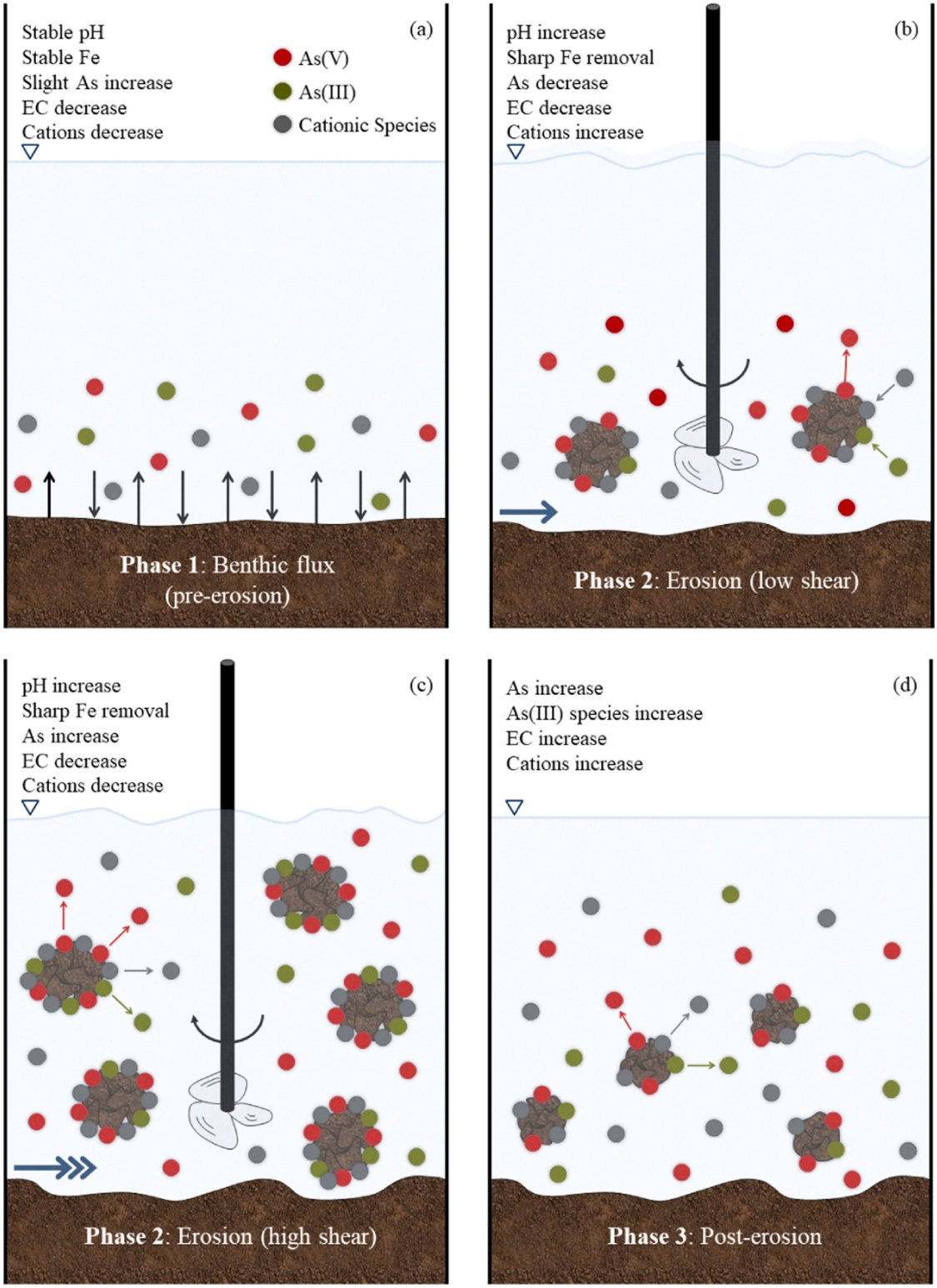

Fig. 5. Schematic presentation of the behavior of As and cationic pollutants before flooding (a), at low shear stress levels (b), at high shear stress levels (c), and after flooding (d).

important intellectual content. **Izaditame, Siebecker, Sparks:** final approval of the version to be published.

Declaration of Competing Interest

The authors declare that they have no known competing financial interests or personal relationships that could have appeared to influence the work reported in this paper.

Acknowledgements

This research is a part of the Delaware EPSCoR's (Established

Program to Stimulate Competitive Research) Project WiCCED (Water in the Changing Coastal Environment of Delaware) supported by the National Science Foundation. The work was financially supported by the National Science Foundation EPSCoR Grant No. 1757353, the Multistate State Hatch Project, NC1187, and the State of Delaware. The authors thank Dr. Linda Kalnejais and Dr. Kai Ziervogel, University of New Hampshire, USA, for their generous supply of the EROMES instrument. We appreciate the Delaware Environmental Institute (DENIN), University of Delaware Soil Chemistry group, Caroline Golt for her ICP expertise, Andrew Homsey for site maps, and John Cargill and others of the Delaware Department of Natural Resources and Environmental Control for assistance in gaining permissions for field sampling. We express our gratitude to Dr. Kianoosh Yousefi for his help with the illustrations and final edition. The authors are also grateful to Dr. Ryan Tappero and the National Synchrotron Light Source II (NSLS II) staff for their support.

Appendix A. Supporting information

Supplementary data associated with this article can be found in the online version at doi:10.1016/j.jhazmat.2021.127161.

References

Agency, U. S. E. P Method 3051a: Microwave Assisted Acid Digestion of Sediments, Sludges, Soils, and Oils; Washington, D.C., USA, 1998.

Ankley, G.T., Toro, Di, Hansen, D.M., D. J, Berry, W.J., 1996. Assessing the ecological risk of metals in sediments. Environ. Toxicol. Chem. Int. J. 15, 2053–2055.

Bijlsma, L., Ehler, C.N., Klein, R.J. T., Kulshrestha, S.M., McLean, R.F., Mimura, N., Turner, R.K., 1996. Coastal zones and small islands. Climate Change 1995: Impacts, Adaptations, and Mitigation of Climate Change: Scientific-Technical Analyses. Contribution of Working Group II to the Second Assessment Report of the Intergovernmental Panel on Climate Change, 289–324.

Borch, T., Kretzschmar, R., Kappler, A., Cappellen, P.V., Ginder-Vogel, M., Voegelin, A., Campbell, K., 2010. Biogeochemical redox processes and their impact on contaminant dynamics. Environ. Sci. Technol. 44 (1), 15–23.

Boudreau, B.P., 1997. Diagenetic Models and Their Implementation, Vol. 410. Springer, Berlin.

Bushey, J.T., Driscoll, C.T., Mitchell, M.J., Selvendiran, P., Montesdeoca, M.R., 2008. Mercury transport in response to storm events from a northern forest landscape. Hydrol. Process. Int. J. 22 (25), 4813–4826.

Cantwell, M.G., Burgess, R.M., Kester, D.R., 2002. Release and phase partitioning of metals from anoxic estuarine sediments during periods of simulated resuspension. Environ. Sci. Technol. 36 (24), 5328–5334.

Cantwell, M.G., Burgess, R.M., King, J.W., 2008. Resuspension of contaminated field and formulated reference sediments Part I: evaluation of metal release under controlled laboratory conditions. Chemosphere 73 (11), 1824–1831.

Chen, C., Wang, L., Ji, R., Budd, J.W., Schwab, D.J., Beletsky, D., Cotner, J., 2004. Impacts of suspended sediment on the ecosystem in Lake Michigan: a comparison between the 1998 and 1999 plume events. J. Geophys. Res. Oceans 109 (C10).

Cherry, J.A., Shaikh, A.U., Tallman, D.E., Nicholson, R.V., 1979. Arsenic species as an indicator of redox conditions in groundwater. In: Developments in Water Science, Vol. 12. Elsevier, pp. 373–392.

Couceiro, F., Fones, G.R., Thompson, C.E., Statham, P.J., Sivyer, D.B., Parker, R., Amos, C.L., 2013. Impact of resuspension of cohesive sediments at the Oyster Grounds (North Sea) on nutrient exchange across the sediment–water interface. Biogeochemistry 113 (1–3), 37–52.

Eggleton, J., Thomas, K.V., 2004. A review of factors affecting the release and bioavailability of contaminants during sediment disturbance events. Environ. Int. 30 (7), 973–980.

Gust, G., Müller, V., 1997. Interfacial Hydrodynamics and Entrainment Functions of Currently Used Erosion Devices. Wiley.

Hoozemans, F.M. J., Marchand, M., Pennekamp, H.A. , 1993. Sea level rise: A global vulnerability assessment vulnerability assessments for population, coastal wetlands and rice production on a global scale. H1588.

Masson-Delmotte, V., Zhai, P., Pirani, A., Connors, S.L., Péan, C., Berger, S., Caud, N., Chen, Y., Goldfarb, L., Gomis, M.I., Huang, M., Leitzell, K., Lonnoy, E., Matthews, J. B.R., Maycock, T.K., Waterfield, T., Yelekçi, O., Yu, R., Zhou, B., 2021. Summary for Policymakers. In: Climate Change 2021: The Physical Science Basis. Contribution of Working Group I to the Sixth Assessment Report of the Intergovernmental Panel on Climate Change. Cambridge University Press/UNEP.

Kalnejais, L.H., Martin, W.R., Signell, R.P., Bothner, M.H., 2007. Role of sediment resuspension in the remobilization of particulate-phase metals from coastal sediments. Environ. Sci. Technol. 41 (7), 2282–2288.

Kalnejais, L.H., Martin, W.R., Bothner, M.H., 2010. The release of dissolved nutrients and metals from coastal sediments due to resuspension. Mar. Chem. 121 (1–4), 224–235.

Klinkhammer, G., Heggie, D.T., Graham, D.W., 1982. Metal diagenesis in oxic marine sediments. Earth Planet. Sci. Lett. 61 (2), 211–219.

Korte, N.E., Fernando, Q., 1991. A review of arsenic (III) in groundwater. Crit. Rev. Environ. Sci. Technol. 21 (1), 1–39.

LeMonte, J.J., Stuckey, J.W., Sanchez, J.Z., Tappero, R., Rinklebe, J., Sparks, D.L., 2017. Sea level rise induced arsenic release from historically contaminated coastal soils. Environ. Sci. Technol. 51 (11), 5913–5922.

Lorke, A., Müller, B., Maerki, M., Wüest, A., 2003. Breathing sediments: the control of diffusive transport across the sediment—water interface by periodic boundary-layer turbulence. Limnol. Oceanogr. 48 (6), 2077–2085.

Love, S., Arndt, T., Ellwood, M., 2013. Preparing for tomorrow's high tide recommendations for adapting to sea level rise in Delaware. Sea Level Rise Vulnerability Assessment for the State of Delaware.

Mobasherpour, I., Salahi, E., Pazouki, M., 2012. Comparative of the removal of Pb^{2+}, Cd^{2+} and Ni^{2+} by nano crystallite hydroxyapatite from aqueous solutions: adsorption isotherm study. Arab. J. Chem. 5 (4), 439–446.

Morse, J.W., 1994. Interactions of trace metals with authigenic sulfide minerals: implications for their bioavailability. Mar. Chem. 46 (1–2), 1–6.

Neil, C.W., Lee, B., Jun, Y.S., 2014. Different arsenate and phosphate incorporation effects on the nucleation and growth of iron (III)(hydr) oxides on quartz. Environ. Sci. Technol. 48 (20), 11883–11891.

Percuoco, V.P., Kalnejais, L.H., Officer, L.V., 2015. Nutrient release from the sediments of the Great Bay Estuary, NH USA. Estuar. Coast. Shelf Sci. 161, 76–87.

Roekens, E.J., Van Grieken, R., 1983. Kinetics of iron (II) oxidation in seawater of various pH. Mar. Chem. 13 (3), 195–202.

Sadiq, M., Zaidi, T.H., Mian, A.A., 1983. Environmental behavior of arsenic in soils: theoretical. Water Air Soil Pollut. 20 (4), 369–377.

Saulnier, I., Mucci, A., 2000. Trace metal remobilization following the resuspension of estuarine sediments: Saguenay Fjord, Canada. Appl. Geochem. 15 (2), 191–210.

Shaw, T.J., Gieskes, J.M., Jahnke, R.A., 1990. Early diagenesis in differing depositional environments: the response of transition metals in pore water. Geochim. Et. Cosmochim. Acta 54 (5), 1233–1246.

Simpson, S.L., Apte, S.C., Batley, G.E., 1998. Effect of short-term resuspension events on trace metal speciation in polluted anoxic sediments. Environ. Sci. Technol. 32 (5), 620–625.

Simpson, S.L., Apte, S.C., Batley, G.E., 2000. Effect of short-term resuspension events on the oxidation of cadmium, lead, and zinc sulfide phases in anoxic estuarine sediments. Environ. Sci. Technol. 34 (21), 4533–4537.

Sparks, D.L., Page, A.L., Helmke, P.A., Loeppert, R.H., 2020. Methods of Soil Analysis, Part 3 Chemical methods, Vol. 14. John Wiley & Sons.

Tolhurst, T.J., Riethmüller, R., Paterson, D.M., 2000. In situ versus laboratory analysis of sediment stability from intertidal mudflats. Cont. Shelf Res. 20 (10–11), 1317–1334.

United Nations, 2007. Percentage Of Total Population Living in Coastal Areas. https://www.un.org/esa/sustdev/natlinfo/indicators/methodology_sheets/oceans_seas_coasts/pop_coastal_areas.pdf.

Warnken, K.W., Gill, G.A., Griffin, L.L., Santschi, P.H., 2001. Sediment-water exchange of Mn, Fe, Ni and Zn in Galveston Bay, Texas. Mar. Chem. 73 (3–4), 215–231.

Wengrove, M.E., Foster, D.L., Kalnejais, L.H., Percuoco, V., Lippmann, T.C., 2015. Field and laboratory observations of bed stress and associated nutrient release in a tidal estuary. Estuar. Coast. Shelf Sci. 161, 11–24.

Yamaguchi, N., Nakamura, T., Dong, D., Takahashi, Y., Amachi, S., Makino, T., 2011. Arsenic release from flooded paddy soils is influenced by speciation, Eh, pH, and iron dissolution. Chemosphere 83 (7), 925–932.